

REAL GAS EFFECTS IN HYPERVELOCITY FLOWS OVER AN INCLINED CONE

R.M. KREK, K HANNEMANN\* and D.I. PULLIN

Department of Mechanical Engineering  
 University of Queensland, St. Lucia, Qld. 4067  
 AUSTRALIA

ABSTRACT

We present pressure measurements obtained from experiments on a cone with a half angle  $\theta = 15^\circ$  at angles of incidence  $\beta = 0^\circ$  and  $\beta = 30^\circ$ , in a hypervelocity flow with a nominal Mach number of 5. Three stagnation enthalpies were used,  $H_0 = 6, 27,$  and  $36$  MJ/kg. Also discussed are the results of a one-dimensional model of dissociation/recombination chemistry in the windward flow about a cone at incidence in a hypervelocity stream. The pressure results agree reasonably well with Newtonian theory, Taylor-Maccoll theory and with detailed three-dimensional calculations when the flow is frozen. The one-dimensional model indicates the presence of reaction quenching on the windward surface at high enthalpies. Pressure measurements at high enthalpy indicate unresolved effects of enthalpy on the leeward flow.

1. INTRODUCTION

When the United States Space Shuttle first reentered the Earth's atmosphere, a near catastrophic shift in the center of pressure was encountered. The shift from the design value was so severe, that the aerodynamic surfaces were adjusted to their maximum position in the opposite sense to that of the design setting. One theory suggested to explain this shift in the center of pressure, is the presence in the flow past the shuttle of real gas effects of molecular dissociation/recombination.

To help us understand the basic dissociation phenomena which occur in these three dimensional high enthalpy flows, a simplified model can be used consisting of an inclined cone in a hypervelocity flow of pure Nitrogen. Experimental study of this flow at sufficiently high enthalpy should provide insight into the interaction between nonequilibrium dissociation chemistry and hypervelocity aerodynamics, and thus help to evaluate the influence of real gas effects on the pressure and the heat transfer distributions on the cone.

The expected structure of hypervelocity flow about an inclined cone is shown in figure 1. The conical bow shock is of greatest strength at the windward stagnation plane but weakens with increasing azimuthal angle  $\phi$ . If the angle of incidence  $\beta$ , is sufficiently large, the flow in the plane normal to the cone axis is supersonic. As the flow expands around the cone surface, the fluid may be expected to first accelerate, and then decelerate as it approaches the leeward plane of symmetry. The pressure recovery required at the symmetry plane requires a pair of cross-flow shocks. Owing to the strong entropy gradients along these shocks the vorticity of the shock-processed flow is

greatly enhanced, with the resultant formation of a complex three-dimensional flow containing one or more pairs of streamwise vortices, and possible shock induced separation from the cone surface. This flow structure is essentially inviscid (see Marconi 1989) but will be modified by the presence of shock induced boundary layer separation. We note that for frozen flow at low enthalpy, (ie. constant  $\gamma$ ), the approximately conical flow will contain no dominant length scale.

2. ONE-DIMENSIONAL MODEL

In order to qualitatively understand the interaction between dissociation chemistry and aerodynamic processes occurring in the windward flow past a cone at incidence, we utilize a simple one-dimensional analysis based on the Lighthill-Freeman ideal dissociating gas (Freeman 1958). The equations of motion for a streamtube of varying area-ratio are given by

$$\rho_1 U_1 A_1 = \rho_2 U_2 A_2, \quad (1a)$$

$$(\rho_1 U_1^2 + P_1) A_1 = (\rho_2 U_2^2 + P_2) A_2 + \int P dA_x, \quad (1b)$$

$$\frac{1}{2} U^2 + R_{nn} (\alpha \theta_D + (4 + \alpha) T) = \text{const.}, \quad (1c)$$

$$P/\rho = RT, \quad R = R_{nn} (1 + \alpha), \quad (1d)$$

$$P = \rho_\infty U_\infty^2 (\sin \theta \cos \beta + \cos \theta \sin \beta \cos \phi)^2, \quad (1e)$$

which are respectively the continuity, the momentum, and the energy equations, the equation of state, and the Newtonian pressure. In equations (1a-e),  $P$  is the pressure,  $\rho$  the density,  $U$  is the fluid speed,  $A$  the stream tube area,  $\alpha = [N]/([N] + 2[N_2])$  is the mass fraction of dissociated Nitrogen,  $\theta$  is the half cone angle,  $dA_x$  is the projected area change of the streamtube in the streamwise direction,  $R_{nn}$  is the gas constant for Nitrogen, and subscripts 1 and 2 refer to streamtube stations.

For nonequilibrium dissociation chemistry a Lagrangian equation for  $\alpha$  following a fluid particle is given by the Lighthill-Freeman model (Freeman 1958),

$$d\alpha/dt = \rho C T^{-\eta} \{ (1-\alpha) e^{-\theta_d/T} - \alpha^2 \rho/\rho_d \}, \quad (2)$$

where the term containing  $(1-\alpha) e^{-\theta_d/T}$  gives the  $N_2 + M \rightarrow 2N$  dissociation reaction rate and that containing  $\alpha^2 \rho/\rho_d$  corresponds to the recombination reaction. For  $N_2$  we take  $\theta_d = 113000$  K,  $\rho_d = 130$  g/cm<sup>3</sup>. Values of  $C$  and  $\eta$  differ in the literature but we take  $\eta = -1.5$  and  $C = 2.7 \times 10^{20}$ .

Equations (1-2) were integrated numerically along particle paths in the thin shock layer between the shock and the cone surface. The bow shock was assumed coincident with the cone surface, and a local

\* Present address: DLR. SM-TS, Bunsen Strasse 10, D-3400, Göttingen, West Germany.



two-dimensional tangent-shock approximation was used to approximate particle paths. The model can only be reasonable only over the windward cone surface ( $\phi < 90^\circ$  in figure 1). Some parametric experimentation was performed with the model but presently we discuss some representative calculations. A specific calculation requires cone geometry, incidence  $\beta$ , freestream conditions and the initial shock co-ordinates ( $\phi_0-z_0$ ) of a particle path (figure 1). The calculation is ended when either the particle reaches a point on the leeward surface where the Newtonian pressure is zero, or when the particle reaches the base plane of the cone. Dissociation is assumed frozen through the shock. All stagnation and freestream conditions used match those found in the experiments, and are given in Tables 1-2. For the case  $H_0 = 6$  MJ/kg the flow everywhere is in chemical equilibrium ( $d\alpha/dt = 0$ ) for all cone configurations and  $\alpha$  is approximately zero. Setting  $H_0 = 28$  and  $36$  MJ/kg introduces nonequilibrium effects into the dissociation chemistry. Figures 2 and 3 show plots of  $\alpha$  versus  $x$  - distance along the particle path.

Fixing  $\beta = 30^\circ$  and  $z_0 = 0.03$  m, and varying  $\phi_0$ , we find that that when  $\phi > 40^\circ$ , the flow appears to be chemically quenched, (see figure 2). Close to the shock the dissociation rate is high due to the strong exponential factor in equation (2), which ensures that dissociation cooling is dominant. Passing downstream this effect decreases rapidly, until cooling associated with rapidly decreasing pressure becomes significant. A further drop in temperature decreases the dissociation rate until it becomes insignificant, and since we are dealing with low densities the effects of recombination are negligible. The reaction is then said to be quenched (Stalker 1989). The closer the starting position is to the windward stagnation ray, the greater the level of dissociation before quenching occurs.

Fixing  $\beta = 30^\circ$  and  $\phi_0 = 1^\circ$ , (see figure 3), and increasing  $z_0$ , the level of dissociation increases, but the particle has greater chance of reaching the cone base plane before quenching occurs. Experimentation was also performed by fixing  $\phi_0$  and  $z_0$ , and altering  $\beta$ , and it was found that with increasing  $\beta$ , the level of dissociation increases.

### 3. EXPERIMENTAL PROCEDURE

The experiments were carried out in The University of Queensland's T4 free piston shock tunnel which is capable of achieving the high temperatures and thus the enthalpy conditions which are experienced during reentry. A Nitrogen test gas was used to further isolate the basic dissociation chemical reactions which occur at these high temperatures. The filling conditions which were used for the experiments are given in Table 1. At  $H_0 = 6.42$  MJ/kg the flow in the test section is expected to be in chemical equilibrium with the two higher enthalpies producing nonequilibrium conditions.

$H_0$ MJ/kg	$P_S$ kPa $N_2$	$P_C$ kPa He	$P_R$ MPa
6.42	80.0	20.2	1.6
27.98	10.0	19.4	2.0
35.82	5.0	19.4	2.0

Table 1 Shock Tunnel Conditions,  $H_0$ - Stagnation Enthalpy,  $P_S$ - Shock Tube Fill Pressure,  $P_C$ - Compression Tube Fill Pressure,  $P_R$ - Reservoir Fill Pressure.

From knowledge of the filling conditions for the shock tunnel, we are able to estimate the freestream conditions in the test section by using the programs ESTC and NENZF. ESTC (Equilibrium Shock Tube

Calculation) is a program which calculates the conditions at the end of the shock tube in the stagnation region (McIntosh 1968). NENZF (NonEquilibrium Nozzle Flow) calculates the conditions in the nozzle as it expands to the freestream conditions, (Lordi et al 1966). These conditions are presented in Table 2.

$H_0$ MJ/kg	$T_\infty$ K	$P_\infty$ kPa	$\rho_\infty$ kg/m <sup>3</sup>	$u_\infty$ km/s	Mach N <sup>o</sup>	$\gamma$	$\alpha_\infty$
6.42	775	5.88	.0256	3.35	5.84	1.4	$\sim 0$
28.0	2560	9.92	.0099	5.67	4.79	1.38	.140
36.0	3518	10.05	.0076	6.17	4.49	1.44	.268

Table 2 Freestream Conditions in Test Section Calculated from NENZF and ESTC

In the freestream  $\alpha$  is not zero for  $H_0 = 28$  MJ/kg and  $H_0 = 36$  MJ/kg, because the temperature reached in the stagnation region of the shock tube is sufficiently high that there is a significant level of dissociated Nitrogen atoms present. When this flow is expanded through the nozzle, freezing of the flow occurs, with a finite level of dissociated atoms present, but the flow is not in local chemical equilibrium. When the flow is processed by the bow shock the static temperature rise is such that the equilibrium levels of dissociation for the flows with  $H_0 = 28$  MJ/kg and  $H_0 = 36$  MJ/kg are  $\alpha_{equil} = 0.965$  and  $\alpha_{equil} = 0.996$  respectively. This indicates that dissociation/recombination chemistry is operative.

The cone used for the experiments had a half angle  $\theta = 15^\circ$  and an axial length 180 mm. The Reynolds number per metre  $Re = \rho u / \mu$ , based on freestream conditions, for the three enthalpy conditions of Tables 1-2 were 2.51, 0.69,  $0.49 \times 10^6$ , respectively, where  $\mu(T)$  is calculated by extrapolating a power law for Nitrogen as given by Hirschfelder et al (1954). The instrumentation on the cone consisted originally of ten Entram pressure transducers and ten Pt-PtRd thermocouple heat transfer gauges. Both the pressure transducers and the thermocouples were mounted in rows of five gauges each, with the rows equispaced around the cone. The arrangement of the cone and its instrumentation is shown in figure 1. Due to pressure transducer problems, we were only able to obtain five gauges that had sufficiently fast response time, such that when normalised against the stagnation pressure, they gave a steady time from which a reasonable level of pressure could be obtained. Steady time is taken when the cone surface pressures normalised on stagnation pressure give a region with a value that is approximately constant. With only five pressure transducers, we could only have one row of transducers. Therefore the cone had to be rotated the full  $180^\circ$ , in increments of  $15^\circ$ .

To establish the uniformity of the flow in the test section, pitot rake measurements were taken for the above three conditions. These experiments were also done in order to compare the pitot pressure readings with those calculated from NENZF. A further reason for performing these experiments is to enable presentation of the cone pressure data normalized to the pitot pressure.

### 4. PRESSURE RESULTS

The results from the calibration experiments at  $\alpha = 0^\circ$  are displayed in figure 4 which show plots of  $P_C/P_{pitot}$  versus cone position for the conditions with  $H_0 = 6.42$  MJ/kg and  $H_0 = 27.98$  MJ/kg. The experiments are compared with Taylor-Maccoll solutions, for which an appropriate value of  $\gamma$  is required. For the equilibrium case, it was found that the flow is



vibrationally frozen, and that we can take  $\gamma = 1.4$ . For  $H_0 = 27$  MJ/kg, the flow is relaxing vibrationally and we take  $\gamma = 4 + \alpha/3$ , assuming ideal dissociating gas behaviour. Figure 4a shows that the measured  $P_c/P_{pitot}$  agrees quite well with the Taylor-Maccoll solution when  $H_0 = 6$  MJ/kg. The average of the experiments differs by 5% from the Taylor-Maccoll theory. For the non-equilibrium case, figure 4b, the average value of the pressure signals is 22% below that of the Taylor-Maccoll value. Apart from the discrepancy in figure 4b, it can be seen that the pressure on the cone surface during the experiment at zero incidence, for both enthalpies is approximately constant along a ray.

Now consider the results obtained from experiments for  $\alpha = 30^\circ$ . Figures 5-7 show  $\ln(P_c/P_\infty)$  versus  $\phi$  at each of the five measuring stations, for  $H_0 = 6, 27$  and  $36$  MJ/kg, respectively. To convert measurements to  $P_c/P_\infty$ , we write  $P_c/P_\infty = P_c/P_{pitot} \times P_{pitot}/P_\infty$ , where  $P_c/P_{pitot}$  are the measured values from experiments. To calculate  $P_\infty/P_{pitot}$ , we assume the pitot pressure is given by,

$$P_{pitot} = 0.93 \rho_\infty U_\infty^2, \quad (3)$$

where  $P_\infty$ ,  $\rho_\infty$ , and  $U_\infty$  are taken from Table 2. This gives  $P_\infty/P_{pitot} = 0.022$ , for  $H_0 = 6$  MJ/kg. Sanderson (private communication, 1989) measured static pressure on a flat plate aligned with  $U_\infty$  at  $H_0 = 6$  MJ/kg. Assuming that this pressure is equal to  $P_\infty$ , Sanderson's measurements give  $P_\infty/P_{pitot} = 0.023$ .

The experiments are compared with the Newtonian estimate for pressure, which in the hypersonic limit and assuming perfect gas behaviour, is given by,

$$P_c/P_\infty = \gamma M_\infty^2 (\sin \theta \cos \beta + \cos \theta \sin \beta \cos \phi)^2 + 1. \quad (4)$$

Figure 5 also shows results obtained from detailed three-dimensional calculations performed by Macrossan *et al* (1989), and these compare favourably with experiments. For all enthalpy cases it can be seen that the Newtonian value of pressure for the first  $60^\circ$  of the windward surface is higher than the values derived from experiments. At  $\phi = 0^\circ$ , the Newtonian values are 4, 6.5, and 7.7 % higher than experiments for  $H_0 = 6, 27$ , and  $36$  MJ/kg respectively. For the equilibrium case, figure 5, better agreement between the Newtonian value and experiments is expected.

The main aim of this project is to investigate the effects of real gas chemistry on the leeward surface of the cone. From figures 5 and 6 it can be seen that the data provides some evidence that cross-flow shocks are occurring on the leeward surface, as suggested in figure 1. The cross-flow shocks occur at about  $\phi = 150^\circ$ , but the resolution of the plots and the

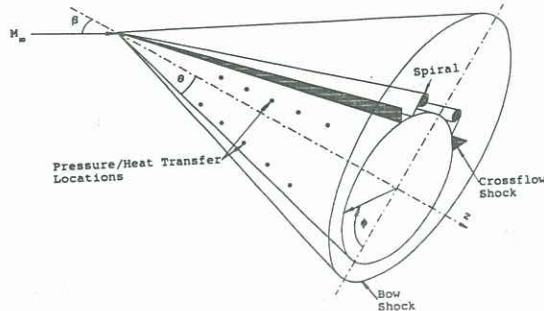


Figure 1: Flowfield for a cone at incidence in a hypervelocity flow.  $\theta$  - half cone angle,  $\beta$  - angle of incidence,  $\phi$  - azimuthal angle,  $z$  - axial distance.

reliability of the pressure gauges make any conclusive quantitative assessment of the results difficult. It is proposed that further experiments on the leeward surface of the cone be conducted using more sensitive pressure gauges, and that a finer survey of the leeward surface be taken. This should allow accurate measurement of the azimuthal position of cross-flow shocks.

## 5. CONCLUSIONS

The one-dimensional model indicates that for the present combination of stagnation enthalpy, freestream conditions and body geometry, quenching of the flow can occur when the flow has expanded to  $\phi > 40^\circ$  around the cone surface. Generally, the longer the particle stays within the high temperature region associated with the windward stagnation portion of the cone, the higher the level of dissociation before quenching occurs, if it does indeed occur.

The pressure results show that the experimental results for  $0^\circ$  and  $30^\circ$  incidence are somewhat lower than their respective Taylor-Maccoll and Newtonian solutions. However reasonable agreement with the detailed calculations of Macrossan *et al* (1989) was obtained for the frozen flow at 6 MJ/kg. We believe the pressure measurements indicate that real gas effects have little influence on the gas dynamics in the windward portion of the cone surface. Calculations of Macrossan *et al* (1989) seem to show a substantial real gas effect on the position of the leeward cross-flow shock, but freestream conditions used in the simulations were somewhat different to those of the present experiments. Further detailed measurements of pressure in the leeward surface are required to investigate this possible effect for the flows at the present high enthalpy conditions.

## REFERENCES

- Freeman, N.C., 1958, *J. Fluid Mech.*, 4, 407-425.
- Hirschfelder, J.O., Curtiss, C.F., & Bird, R.B., 1954., *Molecular Theory of Gases and Liquids.*, John Wiley & Sons, INC., New York.
- Lordi, J.A., Mates, R.E., & Moselle, J.R., 1966, NASA CR-472.
- Macrossan, M.N., Pullin, D.I. & Richter, N.J., 1989, Submitted to 10<sup>th</sup> AFMC.
- Marconi, F., 1989, *J. Comp. and Fluids*, 17, 151-163.
- McIntosh, M.K., 1968, *Computer Program for the Numerical Calculation of Frozen and Equilibrium Conditions in Shock Tunnels.*, Report, Dept. of Physics, ANU, 1968.
- Stalker, R.J., 1989, *Ann. Rev. Fluid Mech.*, 21, 37-60.

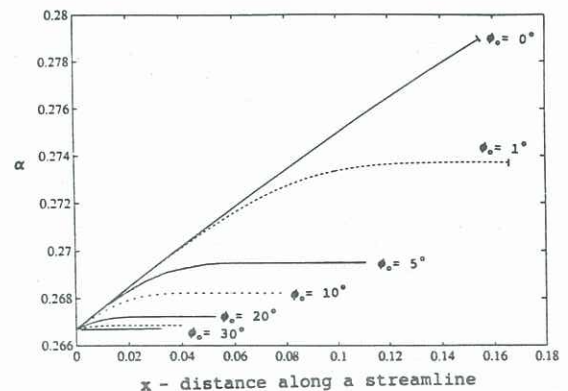


Figure 2:  $\alpha$  versus distance along particle path  $x$  for  $H_0 = 36$  MJ/kg,  $z_0 = 0.03m$ ,  $\beta = 30^\circ$ , varying  $\phi_0$ ,  $\downarrow$  denotes particle reaching cone base plane.

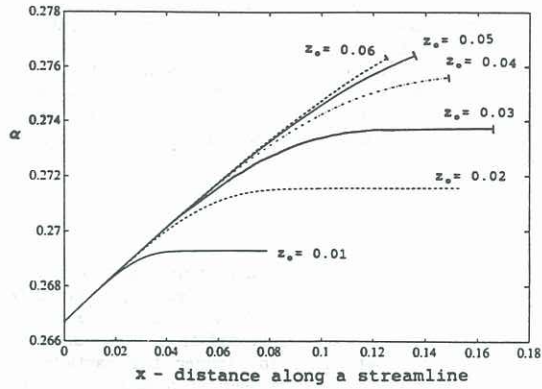


Figure 3:  $\alpha$  versus distance along particle path  $x$  for  $H_0 = 36$  MJ/kg,  $\phi_0 = 1^\circ$ ,  $\beta = 30^\circ$ , varying  $z_0$ ,  $\downarrow$  denotes particle reaching base plane.

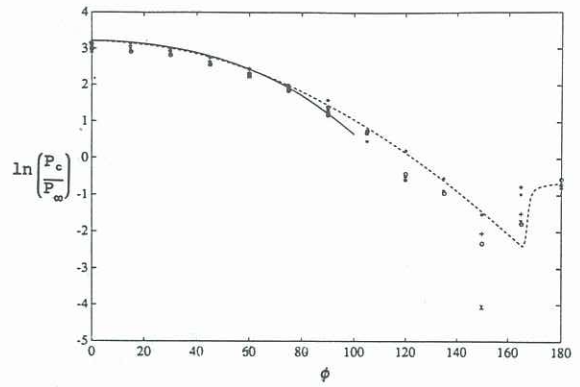


Figure 5:  $\ln(P_c/P_\infty)$  versus  $\phi$ ,  $\beta = 30^\circ$ ,  $H_0 = 6$  MJ/kg, . Position 1, + Position 2, x Position 3, \* Position 4, o Position 5, --- Macrossan et al 1989, — Newtonian.

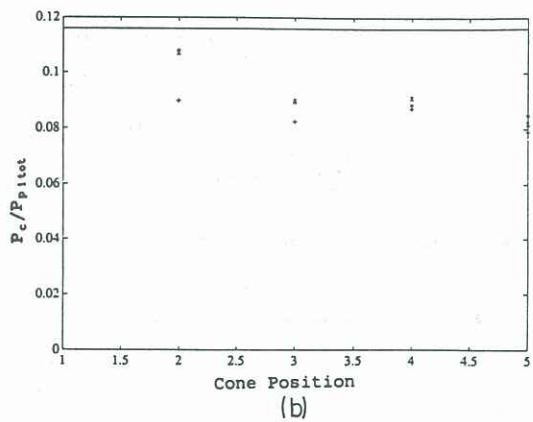
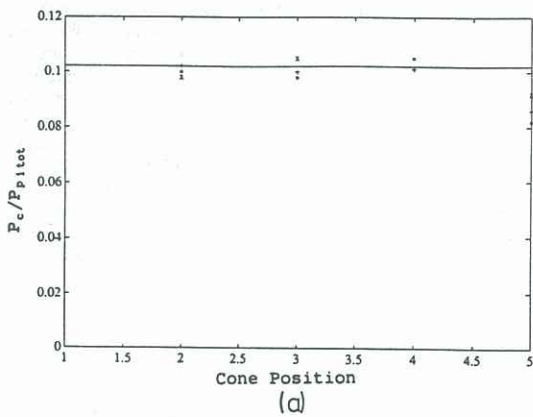


Figure 4:  $P_{c\text{cone}}/P_{\text{pitot}}$  versus cone position for  $\beta = 0^\circ$ ,  
 (a)  $H_0 = 6$  MJ/kg,  $\gamma = 1.4$ ,  $M = 5.84$ ,  
 + s500, \* s501, x s502,  
 — Taylor-Maccoll solution,  
 (b)  $H_0 = 27$  MJ/kg,  $\gamma = 1.38$ ,  $M = 4.79$ ,  
 + s503, \* s511, x s512,  
 — Taylor-Maccoll solution.

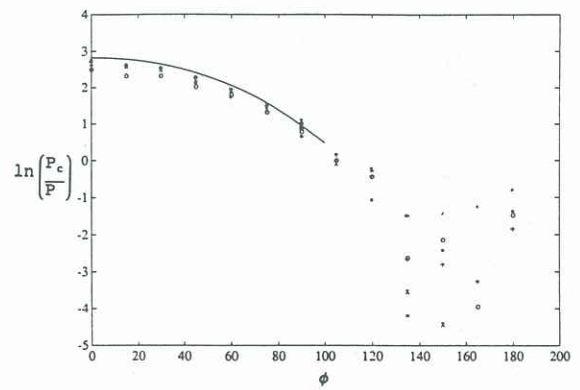


Figure 6:  $\ln(P_c/P_\infty)$  versus  $\phi$ ,  $\beta = 30^\circ$ ,  $H_0 = 27$  MJ/kg, . Position 1, + Position 2, x Position 3, \* Position 4, o Position 5, — Newtonian.

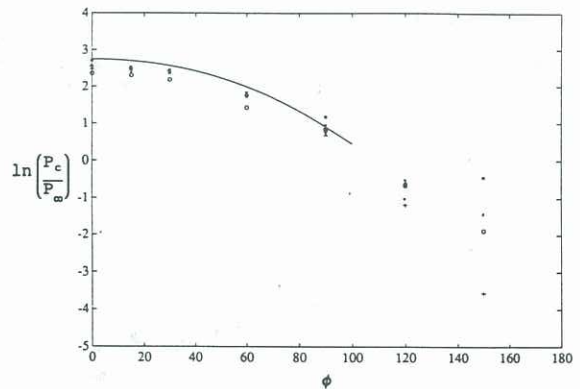


Figure 7:  $\ln(P_c/P_\infty)$  versus  $\phi$ ,  $\beta = 30^\circ$ ,  $H_0 = 36$  MJ/kg, . Position 1, + Position 2, x Position 3, \* Position 4, o Position 5, — Newtonian.